THE ASTROPHYSICAL JOURNAL, 493:91–101, 1998 January 20

ASCA OBSERVATIONS OF TYPE 2 SEYFERT GALAXIES. III. ORIENTATION AND X-RAY ABSORPTION

T. J. TURNER,[1,2] I. M. GEORGE,[1,2] K. NANDRA,[1,3] AND R. F. MUSHOTZKY[1]
Received 1997 April 29; accepted 1997 September 2

ABSTRACT

We discuss the spectral properties of a sample of type 2 Seyfert galaxies based upon the analysis of *ASCA* data. In this paper, we consider the sources for which the X-ray spectra appear to be dominated by the nuclear continuum, transmitted through a large column of absorbing material.

We find that both Seyfert 2 galaxies and narrow emission line galaxies (NELGs) show iron Kα line profiles indicative of reprocessing of nuclear X-rays in a face-on accretion disk. Such line profiles are also observed in Seyfert 1 galaxies. This result is contrary to unification models, which would predict the inner regions of transmitted Seyfert 2 galaxies to be observed edge-on. This raises some questions as to the orientation of the circumnuclear absorber. If the observed differences between Seyfert 1 and 2 galaxies and NELGs are not due to differences in the orientation of the absorbing material, then we suggest that differences in dust composition and grain size, and in the density of the circumnuclear gas, could be of primary importance.

Subject headings: galaxies: active — galaxies: nuclei — galaxies: Seyfert — X-rays: galaxies

1. INTRODUCTION

The classification of an active galactic nucleus (AGN) depends upon the wavelength at which one observes. Historically, optical observations yielded the categories of Seyfert galaxies types 1 and 2, classifying most of the sources that are now "famous." Seyfert 2 galaxies differ from type 1 in that the former show only narrow emission lines in their optical spectra. It was soon realized that some Seyfert galaxies show weak, broad components along with the narrow emission lines, and consequently the subclasses, Seyfert 1.5, 1.8, and 1.9 galaxies, were introduced to quantify the differences in strength of the broad-line components relative to the narrow lines. Narrow emission line galaxies (NELGs) are bright and variable X-ray sources, discovered in early X-ray sky surveys (Marshall et al. 1979). The narrow optical emission lines often have weak, broad Hα and Pβ emission (Ward et al. 1978; Veron et al. 1980; Shuder 1980), making the optical spectra similar to Seyfert 1.9 galaxies. Thus, the NELG classification indicates that the source was discovered in an X-ray survey, but many NELGs are otherwise indistinguishable from Seyfert 1.9 galaxies. Optical spectroscopy and spectropolarimetry, infrared spectroscopy, X-ray spectroscopy, and temporal studies plus γ-ray spectra are all important in the determination of the fundamental nature of obscured nuclei.

Unification models for AGNs postulate that large amounts of dense, molecular material exists between the broad emission line region (BLR) and the narrow emission line region (NLR), in some cases within parsecs of the active nucleus (see Antonucci 1993 for a review of unified models for AGNs). The simplest geometry consistent with observations is a torus, and consequently it has been suggested that one of the primary factors in Seyfert classification is the orientation of the absorbing torus to our line of sight. This hypothesis is consistent with the existence of circumnuclear molecular gas suggested by absorption measurements in a number of wave bands (e.g., Braatz et al. 1993; Greenhill et al. 1996). In unified models, sources observed within the opening angle of the torus correspond to those classified optically as type 1 AGNs, while sources with lines of sight intersecting the torus correspond to type 2 AGNs. Nevertheless, in the latter case, the nuclear light can be observed via scattering or transmission. Antonucci & Miller (1985) provided compelling support for this model when they detected broad, Seyfert 1–type emission lines in the polarized optical spectrum of the Seyfert 2 galaxy NGC 1068, and similar results were later obtained for a number of Seyfert 2 galaxies (Miller & Goodrich 1990; Tran, Miller, & Kay 1992). Recently, Veilleux, Goodrich, & Hill (1997) provided further support for the model with their infrared observations of Paβ, Brγ, and Brα lines in many Seyfert 2 galaxies, revealing hidden BLRs that were not always detectable in scattered optical light. Optically thick tori would be expected to result in collimation of nuclear continuum radiation, and imaging of optical emission lines has shown preferential elongation of some narrow-line regions along the radio axis of the AGN (Haniff, Wilson, & Ward 1988). These regions must be ionized by a more intense radiation field than is directly observed, again supporting the unified model (e.g., Pogge 1988; Tadhunter & Tsvetanov 1989). Further support came from *Ginga* X-ray spectra, which show large absorbing columns and iron Kα lines of high equivalent width (EW) (e.g., Awaki et al. 1991).

The *Advanced Satellite for Cosmology and Astrophysics* (*ASCA*) (Makishima et al. 1996) consists of four co-aligned grazing incidence X-ray telescopes (XRTs; Serlemitsos et al. 1995). The focal-plane instruments are two solid-state imaging spectrometers (SISs), each consisting of four CCD chips, providing an effective bandpass $\sim$0.4–10 keV (Burke et al. 1994), and two gas imaging spectrometers (GISs) at the focus of the other two XRTs, providing coverage over $\sim$0.8–10 keV (Ohashi et al. 1996 and references therein).

[1] Laboratory for High Energy Astrophysics, Code 660, NASA Goddard Space Flight Center, Greenbelt, MD 20771.
[2] Universities Space Research Association.
[3] NAS/NRC Research Associate.

The sources presented here were systematically analyzed in the same way as the broad-line Seyfert galaxies presented in Nandra et al. (1997, hereafter N97). The analysis method is also described in Turner et al. (1997a, hereafter Paper I).

In Paper I, we presented the basic data-analysis results from a sample of *ASCA* observations of Seyfert 2 galaxies, i.e., those having predominantly narrow optical emission lines. The original sample of 26 observations of 25 narrow-line AGNs comprised 17 Seyfert 2 galaxies and eight NELGs drawn from the *ASCA* public archive. In Paper I, we found the 0.6–10 keV *ASCA* spectra of a sample of Seyfert 2 galaxies and NELGs to be complex, often containing a heavily absorbed continuum component, a soft X-ray component, and numerous X-ray emission lines. We found the 6–7 keV regime to be dominated by line flux from gas with an ionization state less than Fe XVI. Several sites are expected to produce significant X-ray line emission in AGNs, including the line-of-sight absorber, optically thick material out of the line of sight (both the putative accretion disk and other larger scale systems such as the torus), ionized (scattering) gas, and regions of starburst emission. The absence of a strong 6.4 keV iron line component in starburst galaxies (Ptak et al. 1997) indicates that the presence of such a line is likely to be an indication of nuclear activity. Iron Kα yields the strongest observed X-ray emission line in Seyfert galaxies, and thus it provides an important probe of conditions in the reprocessing material. A discussion of sources dominated by scattered and Compton-reflected X-rays was presented in a second paper (Turner et al. 1997b, hereafter Paper II).

Figure 1 (repeated from Paper II, for ease of reference) shows the equivalent width of the iron K-shell line plotted against a neutral X-ray–absorbing column, $N_{\rm H}$, for the sample sources. Equivalent widths were measured against the continuum component dominating the 6–8 keV range, and based upon the fit to a narrow Gaussian profile (see Paper I for details). The dot-dashed line in Figure 1 denotes the equivalent width of iron Kα predicted to be produced by transmission through a uniform shell of neutral material (with solar abundances subtending 4π to a continuum source of photon index $\Gamma = 2.0$; Leahy & Creighton 1993), where the photon flux $N(E) \propto E^{-\Gamma}$. The dashed line shows the equivalent width predicted via Compton reflection from optically thick material, as a function of $N_{\rm H}$, assuming that only the power law is absorbed. In this case, the reflection is assumed to be produced from the accretion disk with an equivalent width $\sim$230 eV (N97), as typically observed in Seyfert 1 galaxies. Coincidently, 230 eV represents both the maximum equivalent width observed when iron Kα was parameterized as a narrow Gaussian line and the mean equivalent width assuming a relativistic line profile (N97).

Sources can lie significantly above both of these model lines if the direct continuum is hidden but the reprocessed emission is observed, since the line equivalent width is then measured against a suppressed continuum. Consideration of the iron Kα, [O III] λ5007 line and X-ray variability together suggested that NGC 1068, NGC 4945, NGC 2992, Mrk 3, Mrk 463E, and Mrk 273 are dominated by reprocessed X-rays (Paper II). These sources were denoted "group C" (marked with squares on Fig. 1). Sources lying on the "Leahy and Creighton line" were denoted "group A" (marked as circles on Fig. 1). Thus, group A is composed of NGC 1808, NGC 4507, NGC 5252, NGC 6240, ESO 103-G35, IC 5063, NGC 7172, and NGC 7582. (Table 1 shows the group designation of the sources based upon the original sample). Sources with iron Kα equivalent widths lying between that line and the 230 eV line are consistent with Seyfert 1 spectra transmitted through a high absorbing column and are denoted "group B" (marked as stars on Fig. 1). Group B is composed of NGC 526A, NGC 2110, MCG $-$5-23-16, and NGC 7314, which are all NELGs. This classification implies that we see the nuclear component directly in group B, and this is supported by the observation of rapid X-ray variability in their flux (Paper I and Hayashi et al. 1996) and rapid variability of the iron line profile in NGC 7314 (Yaqoob et al. 1996). This division into groups A, B, and C leaves MCG $-$01-01-043, NGC 4968, NGC 6251, E 0449, NGC 5135, and NGC 1667 unclassified, i.e., those with the lowest signal-to-noise ratio in the *ASCA* data. As we will demonstrate, this crude classification of sources yields a useful insight into the relative importance of the regions contributing to the X-ray spectra in several different cases. The distribution of sample sources is shown in Table 2.

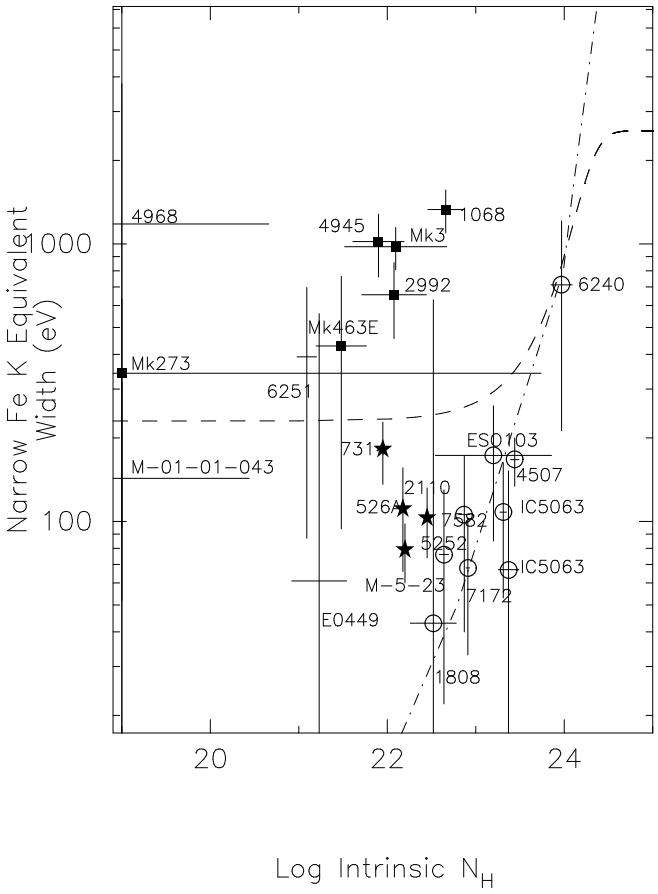

FIG. 1.—EW of the narrow 6.4 keV line vs. absorbing column (from Paper I) for the full sample (excluding NGC 1667, which had a line equivalent width of zero, and NGC 5695, which was not detected). The dot-dashed line shows the line equivalent width expected from a uniform shell of material encompassing the continuum source (Leahy & Creighton 1993). The dashed line shows the predicted equivalent width from reflection as a function of $N_{\rm H}$, assuming that only the power law is absorbed, but that the reflection component remains unchanged. Data points are annotated with an abbreviation of the source name. Group A sources are marked as circles, group B sources as stars, and group C sources as squares. A few of the lowest signal-to-noise ratio data sets have not been classified.

TABLE 1

ASCA SEYFERT 2 SAMPLE

Name (Group)	b/a[a]	R.A.[b]	Decl.[b]	z[c]	Class[d]	N_H (Gal)[e]
MCG −01-01-043	1.0	00 10 03.5	−04 42 18	0.0300	S2	3.27[f]
NGC 526A (B)	0.70	01 23 55.1	−35 04 04	0.0192	NELG	2.33[f]
NGC 1068 (C).....	0.89	02 42 40.8	−00 00 47	0.0038	S2[g,h]	2.93[i]
NGC 1667	0.83	04 48 37.2	−06 19 12	0.0152	S2	5.46[i]
E0449−184	...	04 51 38.8	−18 18 55	0.338	S2	3.73[i]
NGC 1808 (A).....	0.60	05 07 42.3	−37 30 46	0.0033	SB/S2	2.42[i]
NGC 2110 (B).....	0.79	05 52 11.4	−07 27 22	0.0076	NELG	18.60[f]
Mrk 3 (C).....	0.72	06 15 36.3	71 02 15	0.0135	S2[g]	8.70[i]
NGC 2992 (C).....	0.27	09 45 41.9	−14 19 35	0.0077	NELG	5.56[f]
MCG −5-23-16 (B).....	0.45	09 47 40.2	−30 56 54	0.0083	NELG	8.82[i]
NGC 4507 (A).....	0.80	12 35 36.5	−39 54 31	0.0118	S2	7.04[i]
NGC 4945 (C).....	0.13	13 05 26.2	−49 28 16	0.0019	S2[h]	...
NGC 4968	0.47	13 07 06	−23 40 43	0.0100	S2	8.37[i]
NGC 5135	0.80	13 25 44	−29 50 01	0.0137	S2	4.66[i]
NGC 5252 (A).....	0.37	13 38 15.9	04 32 33	0.0230	S1.9	1.97[j]
Mrk 273 (C)	0.27	13 44 42.1	55 53 13	0.0378	S2	1.02[f]
Mrk 463E (C)	0.57	13 56 02.9	18 22 19	0.0500	S2[g]	2.08[i]
NGC 5695	0.73	14 37 22.0	36 34 04	0.0141	S2	1.01[i]
NGC 6251	0.97	16 32 31.9	82 32 17	0.0230	S2	5.48[i]
NGC 6240-49 (A)	0.43	16 52 59.3	02 23 59	0.0245	S2	5.45[i]
ESO 103-G35 (A)	0.51	18 38 20.2	−65 25 42	0.0133	S2/NELG[h]	...
IC 5063 (A)	0.67	20 52 02.9	−57 04 14	0.0113	S2[k]	...
NGC 7172 (A).....	0.42	22 02 02.1	−31 52 12	0.0086	S2/NELG	1.63[f]
NGC 7314 (B).....	0.43	22 35 45.7	−26 03 03	0.0047	S1.9/NELG	1.45[f]
NGC 7582 (A).....	0.46	23 18 23.2	−42 22 11	0.0053	S2/NELG	1.47[f]

NOTE.—Units of right ascension are hours, minutes, and seconds, and units of declination are degrees, arcminutes, and arcseconds.

[a] Inclination, from the NASA Extragalactic Database (NED).
[b] J2000, from NED.
[c] Redshift.
[d] Seyfert type: SB = starburst galaxy, NELG = narrow emission line galaxy.
[e] Galactic H I column density is in units of 10^{20} cm^{-2}.
[f] Stark et al. 1992 and HEASARC.
[g] Polarized broad lines detected (Tran 1995).
[h] Water maser detected (Braatz et al. 1997).
[i] Elvis, Wilkes, & Lockman 1989.
[j] Dickey & Lockman 1990.
[k] Polarized broad lines detected (Inglis et al. 1993).

To summarize, in Paper II we showed that in group C sources the iron Kα complex contains significant contributions from neutral and high-ionization species of iron, thus Compton reflection, hot gas, and starburst emission all could make significant contributions to the observed X-ray spectra. Mrk 3 appeared to be the only source that had little contamination by starburst activity, and in this case the *ASCA* spectrum below 3 keV is dominated by gas with an X-ray ionization parameter $U_X \sim 5$ (as defined by Netzer 1996) and effective column density $N_H \sim 4 \times 10^{23}$ cm^{-2}. This material is more highly ionized than the zone of material comprising the warm absorber seen in Seyfert 1 galaxies (George et al. 1997b, hereafter G97) but may contain a contribution from shock-heated gas associated with the jet.

TABLE 2

POPULATION OF THE GROUPS

Type	A	B	C	Unclassified
NELG/S1.9[a].....	4	4	1	...
Seyfert 2	4	...	5	7
Seyfert 1[b]	...	18	...	...

[a] Objects with both NELG and S2 classifications in the literature are designated as NELGs here.
[b] N97, this entry is included as a reminder that the B class is defined by the properties of Seyfert 1 galaxies.

In this paper, the X-ray properties of sources in groups A and B are examined in the context of unified models for AGNs.

2. CONSTRAINTS FROM EMISSION

2.1. *Continuum Form*

Paper I suggested that the underlying continuum has a power law with a slope $\Gamma \sim 1.9$–2.0 in the 0.6–10 keV band. However, this result might not be meaningful for sources where we used a power law to parameterize a spectrum dominated by scattered or reflected components (i.e., group C). Taking groups A and B, and considering the continuum component that dominates the 2–10 keV band, we obtained weighted mean slopes $\Gamma_A = 1.68 \pm 0.06$ and $\Gamma_B = 2.11 \pm 0.03$, respectively, and a dispersion of 0.11 for group A and 0.31 for group B.

It is difficult to make a strict comparison between our results and the indices derived for Seyfert 1 galaxies. A slope $\Gamma \sim 2$ was obtained when the latter were fitted to a model that included the effects of Compton reflection (e.g., G97). Seyfert 2 galaxies generally have complex soft X-ray spectra, and it is difficult to constrain the soft component, primary power law and the effects of Compton reflection by

using *ASCA* data. However, we can compare the power-law parameterization of the 2–10 keV data with a similar parameterization of Seyfert 1 galaxies. Group A slopes are consistent with the $\Gamma \sim 1.7$ slopes obtained when proportional counter spectra of Seyfert 1 galaxies were modeled with a simple absorbed power law (Mushotzky 1984; Turner & Pounds 1989) over the $\sim$2–10 keV range. Thus, group A appears consistent with the spectra of Seyfert 1 galaxies when a comparison is made between similar fits.

In group B, NGC 526A and NGC 7314 show a flattening of the *ASCA* spectra toward high energies (e.g., Table 12 of Paper I) while the indices inferred for the primary continuum are $\Gamma \simeq 1.8$ and $\Gamma \simeq 2.4$, respectively. MCG -5-23-16 and NGC 2110 appear to be dominated by $\Gamma \simeq 1.9$ and 1.6 components. The $\Gamma \sim 2.4$ slope is the only one that lies outside of the range of slopes observed in the Seyfert 1 sample (G97). However, the slope implied in the case of NGC 7314 depends strongly upon whether or not a hard component is allowed. We conclude that groups A and B both show spectra that are generally consistent with the distribution of primary continuum slopes observed in Seyfert 1 galaxies. Comparing historical X-ray observations of various sources, it seems that some sources show significant index variability, as noted by Weaver et al. (1997) for MCG -5-23-16.

2.2. *Iron* Kα *Line Profiles*

As discussed in § 1, most of the sources in the original sample (of 26 observations) show a significant iron Kα line, and the mean rest energy of the line is 6.40 ± 0.02 keV (Paper I). The equivalent widths from the narrow Gaussian model are shown in Figure 1. Consideration of the (weighted mean) equivalent widths in the narrow Gaussian model to the line yields 113 ± 19 and 97 ± 14 eV for groups A and B, respectively. However, the narrow Gaussian model (with energy fixed at 6.4 keV) could miss some of the flux from a broadened line. The broad Gaussian model yields EWs 153 ± 40 and 223 ± 45 eV for A and B, respectively. The line energies and widths are $E_{\rm A} = 6.37 \pm 0.05$ keV, $\sigma_{\rm A} = 0.21 \pm 0.07$ keV and $E_{\rm B} = 6.33 \pm 0.05$ keV, $\sigma_{\rm B} = 0.32 \pm 0.08$ keV. To investigate further, we constructed average profiles for each group.

Papers I and II show the average SIS + GIS iron Kα line profiles for the individual sources. However, the SIS data have superior energy resolution to the GIS data, and so an examination of the averaged SIS0 + SIS1 data can give the clearest insight into the intrinsic line profiles. Obviously, consideration of the SIS data alone results in a decrease of signal-to-noise ratio when the data are considered on a source-by-source basis. However, the SIS data can provide the most useful information when the data/model ratios for different sources are co-added. The energy scale of each SIS spectrum was redshift-corrected to the rest frame of the source. The average SIS data/model ratio was then calculated (based upon the best-fit continuum model) by combining sources within each group. The result of this summation is shown for each group in Figure 2. The dotted Gaussian profile represents the SIS instrument response for a narrow line observed at a rest energy of 6.4 keV. The profile constructed from the Seyfert 1 sample (N97) is also shown for comparison.

The group C profile shows line flux at and above 6.4 keV (a result that is confirmed by consideration of the fits to the SIS + GIS data for each individual source), probably because of the presence of unresolved iron Kα lines from a range of ionization states (as discussed in Paper II). Interestingly, the group C profile also shows a red wing. While this is small compared with the peak of this line, it is of the same amplitude ($\sim$10%) as that observed in Seyfert 1 galaxies, and group A and B. We return to this point later.

The group B profile is not significantly distinguishable from that observed for Seyfert 1 galaxies (N97). The line peak falls at 6.41 ± 0.02 keV, and the line core is significantly broadened toward lower energies. A very broad wing is also evident, with the broad-line component peaking at 6.44 ± 0.14 keV, with width $\sigma = 0.68 \pm 0.12$ keV.

A broad iron line with a red wing is predicted if the line arises close to the black hole and is subject to gravitational redshift. The iron Kα emission observed in Seyfert 1 galaxies has been successfully modeled with profiles expected for a line originating in an accretion disk around a black hole (e.g., Tanaka et al. 1995; N97), hereafter denoted a disk line. Unless the disk is observed face-on, kinematic (Doppler) effects cause the blue flux of the line to be enhanced relative to the red wing, contrary to what is observed, hence the requirement for a face-on geometry when the red wing is the dominant feature observed. In the Seyfert 1 case, the iron Kα line profile was interpreted as originating in a relativistic accretion disk inclined close to face-on (the mean inclination of the Seyfert 1 sample was $26^\circ \pm 2^\circ$, for a fit where the emissivity was fixed as a function of radius; N97, Table 5). The similarity in line profiles suggests a comparable orientation for the inner regions of group B sources, which are all NELGs.

The group A profile has a core that is consistent with a narrow Gaussian line, centered at 6.4 keV. The equivalent width of the core is 113 ± 19 eV, which could be produced by transmission of the power-law continuum through columns of $\sim 10^{23}$ cm^{-2} in the line of sight (Fig. 1). However, this profile also has excess flux in the wings of the line, reminiscent of the red wing observed in group B and in Seyfert 1 galaxies. In the light of the group B result, we removed the NELGs from the group A profile (half the group). We found that the Seyfert 2 galaxies alone also yield a similar profile with a broad red wing.

Our finding that groups A and B have similar profiles is an interesting and surprising result since unification models predict the inner regions of Seyfert 2 galaxies to be observed edge-on.

We attempted to fit the iron Kα line in individual sources, using the disk-line model profile of Fabian et al. (1989). That model assumes a Schwarzschild geometry and computes the line profile but not the line strength. In that model, the line emissivity is parameterized by a power law as a function of radius, r^{-q}. Since line and continuum parameters can be correlated, and since the fit depends significantly on the assumptions made, we adopted the same assumptions as those used to fit a large sample of Seyfert 1 galaxies (N97), to allow a meaningful comparison between the two sets of results.

In each case, we assumed that the line originates from a region between 6 and $1000 r_g$, where the gravitational radius $r_g = GM/c^2$ and M is the mass of the black hole. The line emissivity function was assumed to be $r^{-2.5}$. We allow the inclination of the disk relative to the observer to be a free parameter (defined such that $i = 0$ is a face-on disk), along with the normalization of the line. We assume the line energy $E_{\rm K\alpha} = 6.4$ keV in the rest frame of the host galaxy.

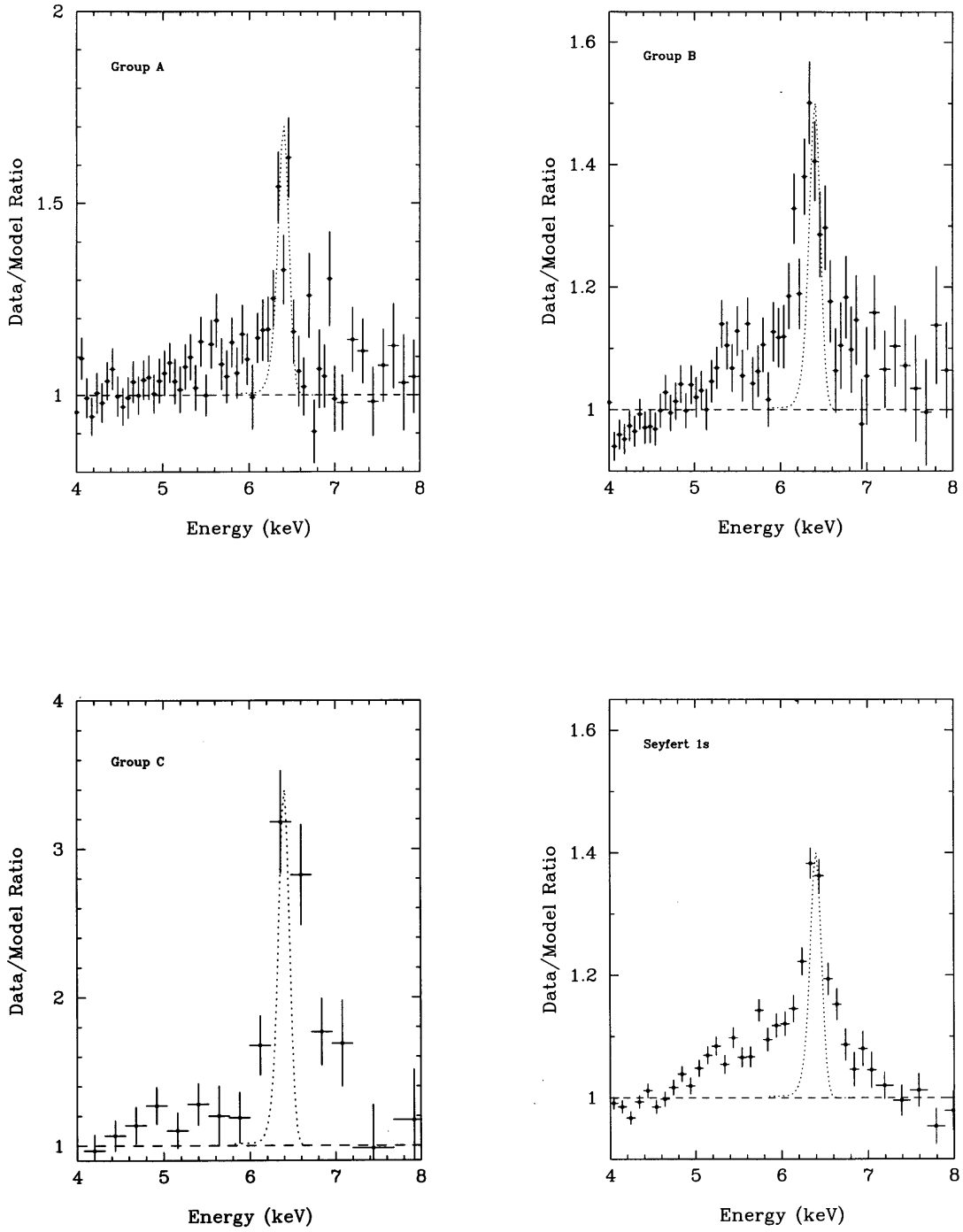

FIG. 2.—The average data/model ratios showing the iron Kα line emission for each group, and that of the Seyfert 1 sample from N97, for comparison. Each data set was corrected to the rest-frame energy before the objects were combined, and so the *X*-axis shows the rest-frame energy. The dotted Gaussian profile represents the SIS instrument response for a narrow line observed at a rest energy of 6.4 keV.

The disk-line fits were performed by assuming the best continuum models from Paper I, with all continuum parameters allowed to be free. The continuum models in Paper I were derived by fitting the 0.6–5.0 plus 7–10 keV data, before consideration of the iron K regime was included in the model. In each case, we also considered the results when an additional (narrow) line component was allowed, to represent the iron line produced in the line-of-sight absorber. The Seyfert 2 galaxies in group A did not generally yield useful constraints on the inclination of any accretion disk system. This is due to the low signal-to-noise ratio in those sources and the allowance of a relatively strong narrow line component in the fits (up to several hundred eV, which could be produced in the line-of-sight absorber). However, fitting a disk-line profile to the bright sources from group B yielded some interesting results. The rest energy of the narrow-line component was fixed at 6.4 keV, and the equivalent width was constrained to be between 10 and 50 eV. This range embraces the values expected from the Leahy & Creighton (1993) simulations but allows a wide range about

the predicted value, to account for differences in spectrum for each source, and possible geometric effects. Errors quoted are 1 σ.

2.2.1. *Disk-Line Fits to Group B Sources*

NGC 526A.—The preferred continuum model for NGC 526A is a double power law with $\Gamma_1 = 1.82^{+0.16}_{-0.14}$, $N_{\rm H} = (1.5 \pm 0.14) \times 10^{22}$ cm^{-2} (Paper I), flattening to $\Gamma_2 = 0.78^{+1.07}_{-0.21}$. Adding a disk-line profile to the model yields an improvement $\Delta\chi^2 = 11$ over the fit to a narrow Gaussian line, with an inclination angle $i = 13^{+6}_{-13}$ degrees and EW = 281 $\pm$ 56 eV. If one assumes instead a single power-law continuum partially covered by the absorber, the fit yields the same inclination and consistent EW = 221 $\pm$ 45 eV for the line. The addition of a narrow Gaussian component (EW $<$ 50 eV) did not significantly improve the fit.

NGC 2110.—The best-fit continuum from Paper I was a $\Gamma = 1.57 \pm 0.07$ continuum partially covered by ionized gas with $U_{\rm X} = 0.006^{+0.62}_{-0.005}$, $N_{\rm H,ion} = 3.9^{+1.71}_{-0.24} \times 10^{22}$ cm^{-2}. The disk line yielded an inclination angle $i = 15^{+9}_{-7}$ degrees, with EW = 289^{+59}_{-52} eV and an improvement $\Delta\chi^2 = 27$ over the fit where the iron Kα line was modeled with a narrow Gaussian component. The addition of a narrow Gaussian component ($<$50 eV) did not significantly affect this fit.

MCG $-$5-23-16.—The nominal best fit from Paper I was $\Gamma_1 = 1.90 \pm 0.04$, $N_{\rm H} = 1.6^{+0.05}_{-0.07} \times 10^{22}$cm^{-2}, steepening to $\Gamma_2 = 4.93^{+0.07}_{-2.08}$ at $\sim$1 keV. A disk-line fit to MCG $-$5-23-16 yielded a reduction $\Delta\chi^2 = 66$ ($F = 60$) compared with the fit where the 5–7 keV band is modeled with a series of narrow lines (Paper I, Table 15). The line EW was 362^{+94}_{-43} eV, and the disk inclination was 33^{+11}_{-4} degrees. The addition of a narrow Gaussian component ($<$50 eV) did not significantly affect this fit. Weaver et al. (1997) found a somewhat higher inclination angle in their analysis of MCG $-$5-23-16, but all disk-line results depend strongly on the assumptions made in the fit, which were different in this analysis versus Weaver et al. (1997). The $i = 33°$ solution is consistent with the observation of some line flux blueward of the peak (in addition to the red wing).

NGC 7314.—The nominal best fit to NGC 7314 was $\Gamma_1 = 2.41^{+0.05}_{-0.05}$, $N_{\rm H} = 1.52^{+0.04}_{-0.14} \times 10^{22}$ cm^{-2}, $\Gamma_2 = 0.97 \pm 0.26$. The addition of a disk-line component yields a good description of the iron Kα line profile, improving the fit by $\Delta\chi^2 = 20$, compared with the narrow Gaussian parameterization. The fit yields $i = 17^{+6}_{-7}$ degrees, EW = 417 $\pm$ 82 eV. The addition of a narrow Gaussian component ($<$50 eV) did not significantly affect this result. However, fits to this source are very sensitive to the underlying continuum and absorption. Fitting the disk line on top of a single power-law continuum, partially covered by a column 8×10^{21} cm^{-2}, produces a solution with $i = 56^{+34}_{-4}$ degrees, EW = 388G $\pm$ 76 eV. The addition of a narrow Gaussian component does not significantly affect this solution. The former fit is nominally statistically preferred (by $\Delta\chi^2 = 13$), but obviously the conclusions drawn depend strongly on the approach taken in the spectral fitting; this is the origin of differences in the results obtained here versus Yaqoob et al. (1996).

2.2.2. *Consideration of the Ubiquity of the Red Wing*

We now consider possible explanations for the ubiquity of the red wing on the iron Kα profiles of Seyfert galaxies.

Given the correlation between line and continuum parameters, an inadequate modeling of the continuum and absorption properties might be misleading us about the profile of the iron Kα line. This is more likely to produce a significant effect in type 2 Seyfert galaxies than in type 1, since the former show relatively large spectral modification due to attenuation in the middle of the *ASCA* bandpass. However, it would be a strange coincidence for such a problem to so closely mimic the profile observed in Seyfert 1 galaxies. Consequently, we consider this possibility unlikely to be the cause of the similarity in observed profiles.

Another possibility is that the type 2 objects have another mechanism for producing a red wing on the iron Kα line. The existence of a Compton shoulder has been suggested for sources such as NGC 1068 (Iwasawa, Fabian, & Matt 1997). However, the Compton shoulder cannot easily produce such a strong wing extending down to such low energies as observed in our profiles.

Despite the systematic effects observed, we note some variety in the profiles of individual sources in the Seyfert type 1 and type 2 samples. We also note that the dark Earth and Coma Cluster do not show these characteristic line profiles in their *ASCA* spectra (N97). These facts suggest that the observed profiles are not an artifact of any outstanding uncertainties with the *ASCA* calibration.

We also consider the possibility that the iron Kα profile is not a good indicator of the orientation of the inner regions of the AGN. If strong relativistic effects bend the light produced close to the central nucleus, then the iron Kα profiles could be distorted, and our fits to a Schwarzchild profile could be misleading as to the orientation of the central source. In particular, the Kerr metric allows contributions to line emission from a disk extending inward to within a few gravitational radii, hence yielding more severely skewed line profiles than are produced around a nonrotating black hole (e.g., Laor 1991). However, these line profiles also have a distinct dependence on inclination angle, and since the line profiles of the type 1 and type 2 Seyfert galaxies are so similar, the preferred orientation of the innermost reprocessor must be the same. In § 4, we investigate the consequences of this conclusion in the context of the unified model.

3. EFFECTS OF OBSCURATION

Observations at different wavelengths provide probes to different depths of the AGN. Assuming the circumnuclear absorbing material has a Galactic dust-to-gas ratio, then a V-band extinction of $A_V = 1$ mag corresponds to a column of neutral hydrogen $N_{{\rm H},z} \sim 1.5 \times 10^{21}$ cm^{-2}. An extinction $A_V < 5$ allows the broad-line region to be observed. $A_V \sim$ 5–8 hides the broad optical lines, and still these AGNs can be identified by direct observation of the Paschen series of lines in the infrared regime. Extinction in excess of $A_V \sim 8$ still allow observations of Paβ (which probe material up to $A_V \sim 11$), Brγ (up to $A_V \sim 24$), and Brα (up to $A_V \sim 63$; see Vielleux et al. 1997). When the extinction approaches $A_V \sim$ 100, then only X-ray and γ-ray observations are able to provide a *direct* view of the nucleus, and as extinction increases beyond this level, then even the 10 keV photons are hidden; the material is optically thick to Compton scattering, and the central source is only detectable via scattering by material out of the line of sight. Thus, the classification assigned to a source may depend on the wavelength at which it is observed. Observations in some bandpasses might not show any signature of an important

component of the system. This has led to some historical confusion as to the nature of some sources.

3.1. *Evidence from ASCA Regarding the Nature of the X-Ray Absorber and Soft Excess*

As evident in Figure 1, the column densities for group B sources are clustered around 10^{22} cm^{-2} while group A spans $\sim 3 \times 10^{22}$–10^{24} cm^{-2}. As discussed in Paper II, the column densities derived for the scattered X-ray sources (group C) generally do not represent the line-of-sight absorption to the nucleus. Group C sources were treated in detail in Paper II, and that class is not discussed further in this section.

Of the sources considered in this paper, only NGC 7172 is consistent with a single power law absorbed by neutral material. The spectra of all the other sources in groups A and B show a strong soft X-ray flux in excess of that predicted by extrapolation of the hard X-ray power law, absorbed by neutral material. A "soft excess" can arise when there are unattenuated lines of sight to the nucleus, when the absorber is ionized, or when a soft emission component is present.

Of the group A sources, NGC 1808, NGC 4507, NGC 6240, ESO 103-G35, and NGC 7582 have an intrinsic 0.5–2.0 keV luminosity in the soft component (alone) $\sim 10^{40}$ ergs s^{-1}, when a correction is made only for the Galactic line-of-sight column. (We note that this yields a lower 0.5–2.0 keV luminosity than those listed in Tables 8–13 of Paper I, which were corrected for total absorption.) Consideration of the maximum starburst contribution to the X-ray flux (Paper I) reveals that only NGC 1808 is consistent with all of that soft flux originating from starburst regions (Tacconi-Garman, Sternberg, & Eckart 1996); however, soft X-ray luminosities $\sim 10^{40}$ ergs s^{-1} could be accounted for by the summed contributions of starburst emission, hot gas, and binary stars in the host galaxy (although, generally, these cannot account for the observed hard X-ray luminosities). No significant variability is evident in the soft flux or absorbing column in NGC 4507, NGC 1808, or NGC 6240 (for which few X-ray observations are available), consistent with an active nucleus covered by a uniform absorber with an extended soft X-ray emission component providing the spectral complexity.

Variations in X-ray absorption have been claimed for ESO 103-G35 (Warwick, Pounds, & Turner 1988) on the basis of two *EXOSAT* observations that revealed a drop in column $\Delta N_{\rm H} = 8 \times 10^{22}$ cm^{-2} in 90 days. The timescale for variability indicated that absorber to be consistent with clouds at a radius coincident with the BLR. The *ASCA* observation reveals an absorbing column consistent with the most heavily absorbed *EXOSAT* spectrum, as does analysis of a later *ASCA* observation (1995 September 26), raising the question as to whether a contaminating source could have affected the apparent measurement of a lower column at one of the *EXOSAT* epochs.

The absorption of NGC 7582 also appears lower ($\Delta N_{\rm H} \sim 1 \times 10^{23}$ cm^{-2}) than that observed during the *EXOSAT* observation (Turner & Pounds 1989). The nearby BL Lac PKS 2316−423 may have contaminated the *EXOSAT* spectrum obtained with the collimated medium-energy (ME) instrument. However, we would expect any such contamination to have made the *EXOSAT* column measurement attributed to NGC 7582 appear lower than the *ASCA* measurement, rather than higher. The nearby clusters Abell 1111S and Sersic 159-03 also posed potential sources of contamination for the *EXOSAT* observations, and could have yielded an erroneous column measurement. Examination of the *EXOSAT* archives shows that the source and background observations had the ME proportional counter offset, with a roll angle designed to minimize the contamination from Sersic 159-03. However, given the large number of contaminating sources in the *EXOSAT* ME field, any claim of column variability in NGC 7582 requires confirmation by using further observations of the source.

In the cases of NGC 526A, NGC 7314, MCG −5-23-16, and NGC 2110 in group B, plus NGC 5252 and IC 5063 from group A, the soft emission exceeds that expected from stellar origins by at least an order of magnitude. These luminous soft components could originate from scattered nuclear flux or leakage of the primary continuum through unattenuated line of sight. In principle, the history of the soft X-ray flux could distinguish between these two. Variations in the absorbing column could indicate that the absorber had a variable ionization state, covering a fraction or column. Analysis of a *ROSAT* HRI observation of NGC 5252 (made in 1995 July) shows the soft flux to be a factor of several lower than that observed by *ASCA* (1994 January). Since the *ASCA* spectrum suggests that the 0.5–2.0 keV flux is dominated by scattered or unattenuated nuclear emission, this variability favors partial covering of the absorber or a subparsec size for the scattering region. Our analysis of the *ROSAT* PSPC observation of IC 5063 shows the soft flux to be consistent with that observed by *ASCA*, allowing no constraint in that case. X-ray column variability has been claimed for NGC 2110 on timescales of years (Hayashi et al. 1996) based upon X-ray observations covering *HEAO 1* (1978) to *ASCA* (1994), although we note that it is difficult to make a conclusive comparison based upon different spectral fits performed across a variety of bandpasses, and that this result needs confirmation. NGC 526A shows strong spectral changes, consistent with column variability, on a timescale of years across five *EXOSAT* observations (Turner & Pounds 1989). Historic X-ray observations of NGC 7314 and MCG −5-23-16 show column measurements consistent with no variation.

A power-law source partially covered by neutral material would be expected to show a leaking fraction with the same spectrum as that observed in the hard X-ray regime. Simple electron scattering of the hard continuum is also expected to yield the same spectrum in scattered X-rays, as the primary continuum. However, many data sets marginally prefer the double power-law model (Paper I), with some sources showing a steep soft X-ray component, and others a hardening of the spectrum toward higher energies. This indicates some spectral curvature that is not accounted for by the aforementioned models. This could be due to curvature in the underlying continuum. However, partial covering by ionized material could also yield a difference in soft and hard spectra. This is the preferred model for Seyfert 1 galaxies (Reynolds 1997; G97) and for NGC 2110 and NGC 5252 from the type 2 sample. Thus, we consider the model in more depth in the next section.

In summary, there is only tentative evidence for column variability in the sample sources. Generally, the spectral shapes can be described by either a continuum attenuated by a patchy or ionized absorber or the presence of a second

emission component. X-ray monitoring of one or more well-chosen Seyfert 2 galaxies will help clarify the picture.

4. DISCUSSION

4.1. *Unification with Seyfert 1 Galaxies—Orientation*

Both of our subsamples of Seyfert 2 galaxies show an iron Kα profile that contains a significant red wing at the same level as that observed in the Seyfert 1 sample. This skewed profile implies that Seyfert 2 galaxies contain an iron Kα line component from a reprocessor close to the central black hole. Furthermore, it is implied that this reprocessor is orientated preferably face-on to our line of sight.

At first sight, this result appears contrary to unification models, which predict that the inner regions of Seyfert 2 galaxies are observed preferentially edge-on. However, in the case of the sources dominated by scattered X-rays (group C), it is likely that the scattering region sees a face-on disk and scatters this spectrum to the observer, whose direct line of sight to the (edge-on) disk is blocked by optically thick material. Thus, results from scattering-dominated sources are in agreement with unification models. Nevertheless, the transmitted X-ray sources, which make up the majority of our sample, also show the signature of a face-on accretion disk, a result that is contrary to unification models. This is particularly interesting in the light of the fact that the host galaxies of Seyfert 2 galaxies are also observed preferentially face-on. Specifically, Kirhakos & Steiner (1990) find the distribution of inclinations to be indistinguishable between type 1 and type 2 hosts when they consider a sample of 288 Seyfert galaxies. Furthermore, both Seyfert type 1 and type 2 samples are observed preferentially face-on compared with a large control sample of normal galaxies. Maiolino & Reike (1995) made a study where the "intermediate" Seyfert 1.8–1.9 galaxies were treated separately from the classical Seyfert 2 galaxies. They found that both Seyfert 1 and Seyfert 2 galaxies are preferentially face-on, but the "intermediate" Seyfert galaxies are preferentially edge-on. This result inferred that the absorption in the Seyfert 1.8–1.9 galaxies might often be due to material in the plane of the host galaxy rather than to circumnuclear material. NELGs are "intermediate" Seyfert galaxies on the basis of their optical properties; however, since the mean iron Kα profiles clearly indicate a preference for a face-on orientation of the inner regions, there cannot be many edge-on sources in our A/B samples or the mean iron Kα profiles would not be so similar to the mean profile for Seyfert 1 galaxies.

To unify groups A and B with Seyfert 1 galaxies, assuming absorption by a torus, would require the torus to be aligned with the accretion disk in Seyfert 1 galaxies, and misaligned in Seyfert 2 galaxies. This problem might be avoided if the absorber is a distribution of clouds, and the type 1 or type 2 nature of a source is simply determined by whether or not a cloud lay across the observers line of sight. Differences in the distribution and composition of the clouds could then account for differences in observed properties. Several Seyfert galaxies vary back and forth between type 1 and type 2 properties on timescales of years. In at least some sources, the observed behavior has been attributed to variations in the reddening, consistent with clouds of dust moving across the line of sight (e.g., Goodrich 1989). The timescales and repetition of this type of behavior argues against both evolutionary models and orientation of large-scale structures of the absorbing material to explain the difference between Seyfert classes, although the "orientation effect" of a cloud being in the line of sight is consistent with the observations.

In the context of cloud models, another possibility is that all classes of Seyfert-type AGNs show a similar mean iron Kα profile because the line is produced by reprocessing in a spherically symmetric distribution of material. Spherical accretion of clouds of material could produce a line showing the strong gravitational effects observed, but with the same profile observed from each viewing direction. The construction of a mean profile for a sample of edge-on Seyfert galaxies, observed directly, rather than in scattered X-rays, would test this theory. The intermediate Seyfert galaxies might provide an edge-on sample. Alternatively, Kirhakos & Steiner (1990) find that *IRAS* galaxies are observed preferentially edge-on. If the orientation of the host galaxy is associated with that of the inner accretion disk/reprocessing region, then *IRAS* galaxies should show an iron Kα profile indicative of edge-on systems, although such a line will be broad and possibly difficult to detect.

We note that the edge-on galaxy NGC 2992 ($b/a = 0.27$) shows an iron Kα line profile with a blue wing (Papers I and II). Weaver et al. (1996) suggest that the large equivalent width of the iron Kα line in NGC 2992 is due to a lag of several years between the direct and reprocessed components. The data are consistent with a narrow component of high equivalent width, as suggested by Weaver et al. (1996), plus a disk-line component from an edge-on accretion disk, which would support a connection between the orientation of the host galaxy and the inner regime. However, the data are also consistent with contributions to the iron Kα line profile from highly ionized species of iron. A search for variability could distinguish between these possibilities, since the occurrence of rapid variability in the blue wing would favor the disk-line scenario.

The existence of "ionization cones" in a dozen or so Seyfert 2 galaxies (e.g., Pogge 1988; Tadhunter & Tsvetanov 1989) poses an interesting problem if we assume the inner regions are viewed with a face-on orientation. Such cones should only be seen in systems observed at a different angle to the escape direction of the radiation. However, many ionization cones are one-sided. This would be expected if we observe close to the direction of the collimated radiation, since one side of the cone will escape in a direction almost directly away from us. In this case, the cone will be foreshortened, and the back side will be heavily absorbed by any intervening Galactic material. We note that one of the best examples of a two-sided cone is in NGC 5252, in which the host galaxy is observed at an intermediate orientation ($b/a = 0.37$).

4.2. *Unification and Absorption*

The fact that observations of the iron Kα line profiles imply a near face-on geometry for the inner regions of both Seyfert 1 and 2 galaxies necessitates a discussion of ways in which factors other than the orientation of the absorbing material can explain the observed differences between the two classes.

The obscuration of the NLR is similar in optically selected Seyfert 1 and Seyfert 2 galaxies, indicating that the obscuration responsible for the differences between these classes is located within the NLR, or out of the line of sight to the NLR (Lawrence & Elvis 1982; De Zotti & Gaskell

1985). In NELGs, the X-ray–absorbing columns are 10^{22}–10^{23} cm^{-2} (NGC 7314 to ESO 103-G35) while the optical lines imply an attenuation less than 7×10^{21} cm^{-2} (assuming a Galactic gas-to-dust ratio). This implies that the X-ray absorber lies within the BLR, or is highly ionized, otherwise it would produce stronger suppression of the BLR than that which is observed.

In Seyfert 2 galaxies, X-ray column densities are 10^{23} cm^{-2} or greater. Extinction of the broad lines occurs for columns in excess of 1×10^{22} cm^{-2}. On this basis, the X-ray absorption in Seyfert 2 galaxies can only be said to exceed that required to fully suppress the broad optical lines, yielding no constraint on the location of the absorber.

Granato, Danese, & Franceschini (1997) compare the infrared broadband spectra and spectroscopy results with *Ginga* X-ray spectra of a sample of Seyfert 2 galaxies (Smith & Done 1996). For convenience, we define the infrared extinction as τ_{IR} and the X-ray extinction as τ_X, where $I_{obs} = I_{int}\, e^{-\tau}$, I_{obs} is the observed flux, and I_{int} is the intrinsic flux. Granato et al. find that the infrared extinction, τ_{IR}, is approximately consistent with the X-ray extinction, τ_X, for columns $\lesssim 10^{22}$ cm^{-2}, while $\tau_{IR} \sim 0.1\tau_X$ for $3 \times 10^{22} < N_H < 10^{24}$ cm^{-2} and $\tau_{IR} \ll 0.1\tau_X$ for $N_H > 10^{24}$ cm^{-2}. Thus, their finding indicates that where there is a large X-ray absorption, the material likely sits predominantly within the dust sublimation radius.

ASCA evidence for an ionized absorber covering NGC 2110 and NGC 5252 makes it interesting to examine the general results from such a model, particularly in the light of the strong evidence for ionized absorbers in most Seyfert 1 galaxies (e.g., Reynolds 1997; G97).

To examine the unification of Seyfert 1 and 2 galaxies, we examined the distribution of column, ionization parameter, and luminosity for both types. We took the Seyfert 1 results from G97. Those sources were analyzed in the same way as our sample of Seyfert 2 galaxies, allowing a direct comparison to be made. Figure 3 shows U_X and N_H, the ionization state and column of ionized material versus (unabsorbed) X-ray luminosity adapted from a figure in G97 (group B sources are marked with stars, group A with circles, Seyfert 1 galaxies with open squares). This comparison demonstrates that while the mean column appears to be higher for type 2, some Seyfert 1 galaxies are also consistent with having large columns of circumnuclear material (which is so highly ionized that it does not provide much opacity below ~ 3 keV).

Examination of Figure 3 shows that there is a large overlap in intrinsic (absorption-corrected) luminosity in the type 2 and type 1 sample sources, although the mean intrinsic luminosity of the Seyfert 2 galaxies is lower. For gas of the same density and distance from the ionizing source, the ionization parameter is, by definition, proportional to the ionizing luminosity. The Seyfert 1 sample appears consistent with $U_X \propto L_X$, and hence the circumnuclear gas is consistent with similar density and location across the type 1 sample. However, Seyfert 2 galaxies are clearly inconsistent with that picture, most notably due to several sources absorbed by material of very low ionization state. We also note that overlaying three quasars on this plot (marked with solid squares; from George et al. 1997a) indicates that there is no simple proportionality between U_X and L_X. This indicates that the absorbing material in Seyfert 2 galaxies exists under significantly different conditions than that in type 1 galaxies. Differences in gas density, geometry, and location between individual objects could cause the observed effects. Seyfert 1 galaxies do not show such pronounced suppression of the broad optical lines as type 2 sources do with the same nuclear (X-ray) luminosity. This indicates systematic differences in the location of the dust sublimation radius between classes of AGNs.

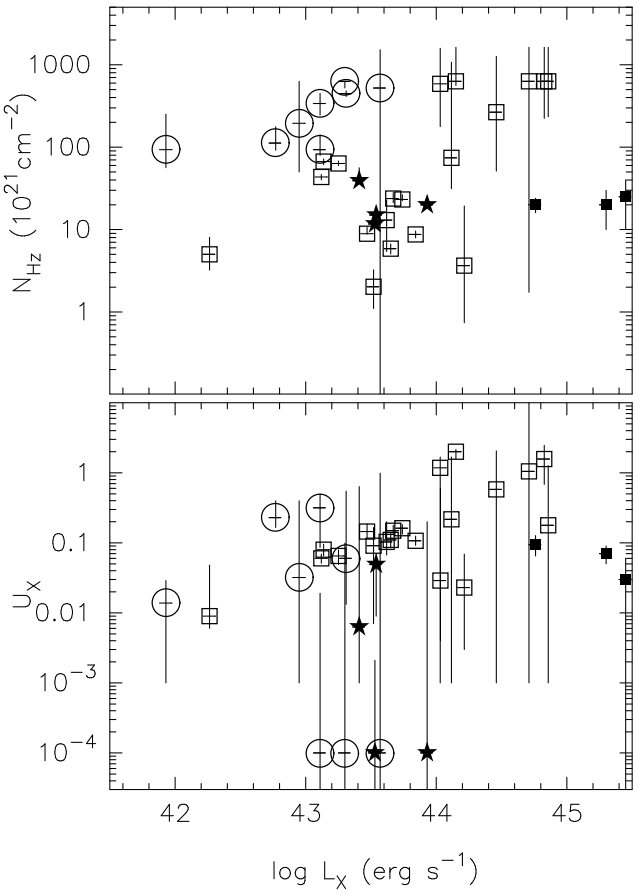

FIG. 3.—The absorption-corrected 2–10 keV luminosity vs. the ionization state and column of the circumnuclear gas, U_X and N_H. The open squares represent the Seyfert 1 sample of G97, the open circles are the group A sources, stars are group B, and the filled squares represent three quasars (see § 4.2).

Reverberation studies have indicated BLR sizes $r_{BLR} \sim 0.02 L_{45}^{0.5}$ pc (Peterson et al. 1993; Netzer 1990), although the BLR probably extends over an order of magnitude in radius (Korista et al. 1995). For bolometric luminosities 10^{43}–10^{44} ergs s^{-1} (appropriate for our sample sources), we estimate the BLR to be 6×10^{15}–2×10^{16} cm (approximately a few light days). Barvainis (1987) shows that the dust sublimation radius $r_{sub} = 0.13 L_{UV44}^{0.5}\, T_{1500}^{-2.8}$ pc, where L_{UV} is the UV luminosity in units of 10^{46} ergs s^{-1} and T_{1500} is the grain sublimation temperature in units of 1500 K. Order-of-magnitude estimates show the dust sublimation radius to lie close to or just outside of the BLR. Barvainis also notes that the highest sublimation temperature occurs for dust composed of graphite grains and is ~ 1500 K. Dust containing silicate grains would have a lower temperature and hence a larger sublimation radius. Evidently, different mixtures of dust grains will allow the sublimation radius to change by up to a factor of a few. The size of the dust grains yields an even bigger effect. Laor & Draine (1993) show that graphite grains of size ~ 10 μm can exist almost an order of magnitude closer to the nucleus than grains of size ~ 0.005 μm.

Thus, differences in the distribution of grain sizes could allow significant differences in the location of r_{sub} relative to the BLR in different sources; r_{sub} will be closer to the nuclei in those sources with the largest dust grains. However, as also shown by Laor & Draine (1993), some distributions of grain size yield dust that is ineffective at reddening, i.e., the effective extinction can have a flat dependence over a large frequency range. The data require that, for Seyfert 2 galaxies, the BLR is deeply situated well within r_{sub}; for NELGs, the BLR is probably very close to r_{sub} because the broad lines suffer some obscuration. Thus, differences in dust content and in the distribution of grain sizes could be the key to unification of Seyfert 1 and 2 galaxies. In fact, Konigl & Kartje (1994) suggested a dusty wind model to unify AGNs, with partially ionized gas in the inner regions of the wind accounting for the bulk of X-ray absorption seen in face-on sources.

Spectral variability in the optical and X-ray regimes could be driven by changes in the nuclear flux, which will move the effective radii of ionization and sublimation. Differences in the distribution of circumnuclear material and in the total mass of gas surrounding the nuclei may also play a role. A model in which clouds of optically thick material cause the X-ray obscuration can explain many observed properties (Guilbert & Rees 1988). The location, size, and column density of the clouds can determine whether column variability or a leaking fraction of nuclear flux is observed. Compton reflection can occur from the surface of the blobs (Nandra & George 1994) while scattering of nuclear radiation can occur from a region of hot gas, so long as there are some unattenuated lines of sight by which to view this. Collimation of radiation (to produce ionization cones) could also occur, if the blobs are distributed around a preferred plane.

Interestingly, Maiolino et al. (1995) find differences in infrared colors, indicating that the host galaxies of type 2 nuclei have significantly higher levels of starburst activity than type 1 nuclei. This starburst activity occurs close to the nucleus, and since starburst regions contain large amounts of dusty gas, perhaps the presence of these starburst regions results in a different gas and dust content in Seyfert 2 galaxies. Thus, we concur with the suggestion of Maiolino et al. that consideration of the starburst regions seems likely to provide an important component of unification models. Differences in the dust content of the circumnuclear gas might also be related to the apparent preferential occurrence of masers in Seyfert 2 galaxies. The relationship between a high X-ray–absorbing column and the existence of water masers in Seyfert 2 galaxies (Braatz, Wilson, & Henkel 1997) indicates that the material in which the maser amplification occurs is related to significant X-ray opacity. *If* the molecular gas is in a well-defined plane, then masers will be preferentially observed in sources viewed within a few degrees of that plane. The sources in our original sample that are known to have masers are NGC 1068, NGC 4945, and ESO 103-G35 (Braatz et al. 1997). NGC 1068 and NGC 4945 are so highly absorbed that the X-ray spectra are seen only in reprocessed photons, and the *ASCA* data are consistent with the high degree of opacity expected from an edge-on masing disk. The signature of a face-on accretion disk in these cases is an indication of the orientation of the scattering material relative to that disk, as discussed earlier. In the case of ESO 103-G35, the inner accretion disk appears to be observed directly, but the *ASCA* data do not allow a useful constraint to be placed on the disk inclination.

5. CONCLUSIONS

Examination of the iron Kα line from a sample of NELGs and Seyfert 2 galaxies shows profiles similar to those observed in Seyfert 1 galaxies, and indicative of an origin in an accretion disk orientated face-on. Unification models predict the inner regions of Seyfert 2 galaxies to be observed edge-on, for sources where we have a direct line of sight to the nucleus. The preference for a face-on orientation of the accretion disk in Seyfert 1 galaxies and transmitted Seyfert 2 galaxies poses some questions as to the orientation and geometry of gas comprising the circumnuclear absorbing material. If the absorber is composed of clouds, then differences in gas density, size of dust grains and dust composition, and the distribution of the clouds seem a likely explanation of the observed differences in the X-ray and optical absorption properties of Seyfert 1 galaxies, Seyfert 2 galaxies, and NELGs. These results indicate that further refinement is required for unified models for AGNs.

We are grateful to the *ASCA* team for their operation of the satellite, and to Keith Gendreau, Tahir Yaqoob, and Ski Antonucci for useful comments. This research has made use of the NASA/IPAC Extragalactic database, which is operated by the Jet Propulsion Laboratory, Caltech, under contract with NASA; of the SIMBAD database, operated at CDS, Strasbourg, France; and data obtained through the HEASARC on-line service, provided by NASA/GSFC. We acknowledge the financial support of the Universities Space Research Association (I. M. G., T. J. T.) and the National Research Council (K. N.).

REFERENCES

Antonucci, R. 1993, ARA&A, 31, 473
Antonucci, R., & Miller, J. S. 1985, ApJ, 297, 621
Awaki, H., Koyama, K., Inoue, H., & Halpern, J. P. 1991, PASJ, 43, 195
Barvainis, R. 1987, ApJ, 320, 537
Braatz, J. A., Wilson, A., Gezari, D. Y., Varosi, F., & Beichman, C. A. 1993, ApJ, 409, L5
Braatz, J. A., Wilson, A. S., & Henkel, C. 1997, ApJS, 110, 321
Burke, B. E., Mountain, R. W., Daniels, P. J., & Dolat, V. S. 1994, IEEE Trans. Nuc. Sci., 41, 375
De Zotti, G., & Gaskell, C. M. 1985, A&A, 147, 1
Dickey, J. M., & Lockman, F. J. 1990, ARA&A, 29, 215
Elvis, M., Wilkes, B. J., & Lockman, F. J. 1989, AJ, 97, 777
Fabian, A. C., Rees, M. J., Stella, L., & White, N. E. 1989, MNRAS, 238, 729
George, I. M., Nandra, K., Netzer, H., Laor, A., Turner, T. J., Mushotzky, R. F., & Fiore, F. 1997a, in preparation
George, I. M., Turner, T. J., Netzer, H., Nandra, K., Mushotzky, R. F., & Yaqoob, T. 1997b, ApJ, submitted (G97)
Goodrich, R. 1989, ApJ, 340, 190
Granato, L. G., Danese, L., & Franceschini, A. 1997, ApJ, 486, 147
Greenhill, L. J., Gwinn, C. R., Antonucci, R., & Barvainis, R. 1996, ApJ, 472, L21
Guilbert, P. W., & Rees, M. J. 1988, MNRAS, 233, 475
Haniff, C. A., Wilson, A. S., & Ward, M. J. 1988, ApJ, 334, 104
Hayashi, I., Koyama, K., Awaki, H., Yamauchi, S., & Ueno, S. 1996, PASJ, 48, 219
Inglis, M. D., Brindle, C., Hough, J. H., Young, S., Axon, D. J., Bailey, J. A., & Ward, M. J. 1993, MNRAS, 263, 895
Iwasawa, K., Fabian, A. C., & Matt, G. 1997, MNRAS, 289, 443
Kirhakos, S. D., & Steiner, J. E. 1990, A&A, 99, 1435
Konigl, A., & Kartje, J. F. 1994, ApJ, 434, 446
Korista, K. T., et al. 1995, ApJS, 97, 285

Laor, A. 1991, ApJ, 376, 90
Laor, A., & Draine, B.T. 1993, ApJ, 402, 441
Lawrence, A., & Elvis, M. E. 1982, ApJ, 256, 410
Leahy, D. A., & Creighton, J. 1993, MNRAS, 263, 314
Maiolino, R., & Rieke, G. H. 1995, ApJ, 454, 95
Maiolino, R., Ruiz, M., Rieke, G. H., & Keller, L. D. 1995, ApJ, 446, 561
Makishima, K., et al. 1996, PASJ, 48, 171
Marshall, F. E., Boldt, E. A., Holt, S. S., Mushotzky, R. F., Rothschild, R. E., Serlemitsos, P. J., & Pravdo, S. H. 1979, ApJS, 40, 657
Miller, J. S., & Goodrich, R. W. 1990, ApJ, 355, 456
Mushotzky, R. F. 1984, Adv. Space Res., 3(10–12), 157
Nandra, K., & George, I. M. 1994, MNRAS, 267, 974
Nandra, K., George, I. M., Mushotzky, R. F., Turner, T. J., & Yaqoob, T. 1997, ApJ, 477, 602 (N97)
Netzer, H. 1990, in Saas-Fée Advanced Course 20, Active Galactic Nuclei, ed. T. J. L. Courvoisier & M. Mayor (Berlin: Springer), 57
———. 1996, ApJ, 473, 781
Ohashi, T., et al. 1996, PASJ, 48, 157
Peterson, B., et al. 1993, PASP, 105, 247
Pogge, R. W. 1988, ApJ, 328, 519
Ptak, A., Serlemitsos, P., Yaqoob, T., Mushotzky, R. F., & Tsuru, T. 1997, AJ, 113, 1286
Reynolds, C. 1997, MNRAS, 286, 513
Serlemitsos, P. J., et al. 1995, PASJ, 47, 105
Shuder, J. M. 1980, ApJ, 240, 32
Smith, D., & Done, C. 1996, MNRAS, 280, 355
Stark, A. A., Gammie, C. F., Wilson, R. W., Bally, J., Linke, R. A., Heiles, C., & Hurwitz, M. 1992, ApJS, 79, 77
Tacconi-Garman, L. E., Sternberg, A., & Eckart, A. 1996, AJ, 112, 918
Tadhunter, C., & Tsvetanov, Z. 1989, Nature, 341, 422
Tanaka, Y., et al. 1995, Nature, 375, 659
Tran, H. D. 1995, ApJ, 440, 597
Tran, H. D., Miller, J. S., & Kay, L. E. 1992, ApJ, 397, 452
Turner, T. J., George, I. M., Nandra, K., & Mushotzky, R. M. 1997a, ApJS, 113, 23 (Paper I)
———. 1997b, ApJ, 488, 164 (Paper II)
Turner, T. J., & Pounds, K. A. 1989, MNRAS, 240, 833
Veilleux, S., Goodrich, R. W., & Hill, G. J. 1997, ApJ, 477, 631
Veron, P., Lindblad, P. O., Zuiderwijk, E. J., Adam, G., & Veron, M. P. 1980, A&A, 87, 245
Ward, M. J., Wilson, A. S., Penston, M. V., Elvis, M., Maccacaro, T., & Tritton, K. P. 1978, ApJ, 223, 788
Warwick, R., Pounds, K. A., & Turner, T. J. 1988, MNRAS, 231, 1145
Weaver, K. A., Nousek, J., Yaqoob, T., Mushotzky, R. F., Makino, F., & Otani, C. 1996, ApJ, 458, 160
Weaver, K. A., Yaqoob, T., Mushotzky, R. F., Nousek, J., Hayashi, I., & Koyama, K. 1997, ApJ, 474, 675
Yaqoob, T., Serlemitsos, P. J., Turner, T. J., George, I. M., & Nandra, K. 1996, ApJ, 470, 27